Corrosion Behavior and Wear Resistance Characteristics of Electroless Ni-P-CNTs Plating on Carbon Steel

Zhiming Gao[*], Song Zhao, Ying Wang, Xin Wang, Lijuan Wen

School of Materials Science and Engineering, Tianjin University, Tianjin 300072, P.R. China
[*]E-mail: gaozhiming@tju.edu.cn

Electroless Ni-P-CNTs plating is used to find the influence regularity of different CNTs concentration on the properties of the composite coating，including corrosion resistance, wear resistance and surface hardness. The results show that CNTs intersperse in the gaps between the deposited metal particles and the size of the metal particles is much smaller than the size of the metal particles which aren't wrapped with CNTs. The codeposition of Ni-P-CNTs can work as a kind of lubricant between the coating and the other friction body. Compared to the Ni-P coating, the wear resistance and the surface hardness value of Ni-P-CNTs coating are better, and they become much better with the increase of the CNTs concentration. The addition of CNTs makes the coating denser, thus compared with Ni-P coating, the corrosion resistance of composite coating is better. But too much CNTs deposited on the substrate occupy the position of the nickel and phosphorus, leading to a large area of the carbon nanotubes wrapped together which is very unfavorable to coating, resulting in the corrosion potential of the composite coating becoming negative gradually, indicating the corrosion resistance of the composite coating becomes worse.

1. INTRODUCTION

Remanufacturing has emerged as a promising practice to reduce the environmental impact of products by extending their lifespan and thus precluding the need for consistent replacements that are costly in terms of both energy consumption and financial expenditure [1]. The remediation technology for remanufacturing parts which become failures by wear, corrosion or breaking is the core of the machinery remanufacturing.

People pay more attention to electroless plating for the good properties of the coating and the simple, energy saving and environmental process. Eletroless plating is suitable for the remediating of

the remanufacturing parts as the coating has excellent corrosion resistance and wear resistance. Researchers started to boost research into composite plating. In the process of electroless plating nanoparticles functioning as enhanced phase were doped with. The composite coating containing nanoparticles whose size scale is 15-50 nm has many properties that the simple metal plating doesn't have, such as better corrosion resistance, better wear resistance and stronger adhesion between the coating and substrate [4-6]. Electroless Ni-P-nanoparticles plating was applied on kinds of materials including metal, polymer and ceramics [7-11]. Carbon nanotubes (CNTs) have a nanoscale diameter. The theoretical Young's modulus is 1.8TPa and the flexural strength is 14.2GPa. CNTs are used to prepare super composite materials for the higher strength and toughness [12]. CNTs are used as enhanced phase to prepare metal and polymer matrix composites [13-16]. The mechanical property is excellent. Because the structure of CNTs is the same as the lamellar structure of the graphite, CNTs have good electrical properties and heat conducting properties. The thermal expansion coefficient of CNTs is almost zero [17-20]. CNTs have higher thermal conductivity. The thermal conductivity of the composite material will improve if the composite material is doped with CNTs [21].

According to literature, Ni–P-CNTs composite coatings exhibit high wear resistance and low friction coefficient [22-24]. However, there are very few reports regarding the corrosion resistance mechanism of the Ni-P-CNTs composite coatings. According to some reports the results indicated that the incorporation of carbon nanotubes in the coating improved both tribological behavior and corrosion resistance [24, 25]. However, some research showed the corrosion resistance of Ni-P-CNTs composite coatings is worse than that of Ni-P coatings without CNTs [26].

To figure out the effect of incorporation of CNTS on the corrosion resistance and the mechanical properties eletroless Ni-P-CNTs plating was used to study this problem and the effect of CNTs concentration on these properties.

2. EXPERIMENTAL

45# steel which is most commonly used in the field of machinery was selected for this study. The chemical composition and mechanical properties of 45# steel are shown in Table 1. The multi-walled CNTs used in this work were prepared in ordinary CVD method, whose diameter is approximately 10-20nm and length 1 μm. Most were in bamboo-like and straight tubular form. The 45# steel was cut into 7×15 mm rectangle samples which were polished by using different types of water sandpaper. Before plating they were degreased with 0.4 M NaOH, 0.4 M $NaCO_3$ and 0.002M Sodium dodecyl sulfate solution at 70 ^{o}C for 30 min. Then they were etched in a 20 mL HCl , 5 mL H_2SO_4 and 70 mL H_2O solution. On top of etching they were activated in a 10% HCl solution for 3 min at room temperature and then washed fully with deionized water.

Table 1. The chemical composition and mechanical properties of 45#

C	Si	Mn	Cr	Ni
0.42-0.50%	0.17-0.37%	0.50-0.80%	≤0.25%	≤0.30%

Yield Strength	Tensile Strength	Elongation	Shrinkage	Impact Energy
355MPa	600MPa	16%	40%	39J

The basic bath for plating of Ni–P binary alloy deposits was as follows: $NiSO_4 \cdot 7H_2O$ （30 g•L^{-1}） ,$NaH_2PO_2 \cdot H_2O$ （40 g•L^{-1}） , sodium citrate （10 g•L^{-1}） , acetic acid （10 ml·L^{-1}） , lactic acid （10 ml·L^{-1}） . Ammonium hydroxide was chosen to adjust the pH of plating bath to 4.5.

The pretreated carbon nanotubes (0 g•L^{-1}, 0.5 g•L^{-1}, 1.5 g•L^{-1}, 2.0 g•L^{-1}) were added to the bath, and then ultrasonic was used to disperse the carbon nanotubes for 15 min. The process was carried out at 85°C with the stirrer stirring for 120 min. After plating the samples were cleaned with cold water for 2 min and then dried.
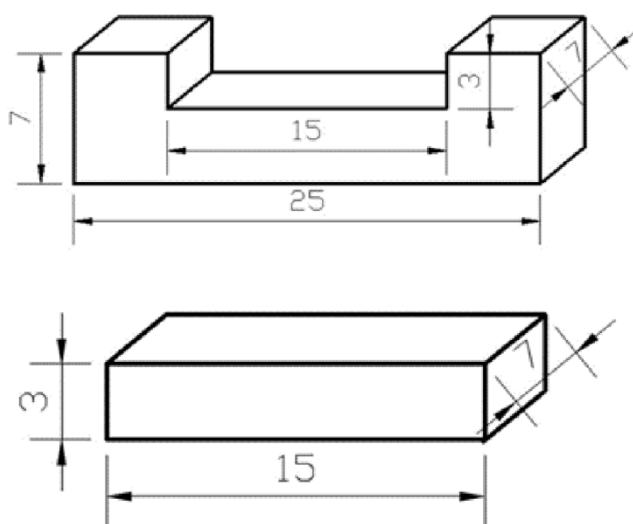
Figure 1. Sample size of friction-abrasion testing (unit: mm)

The microhardness of the plating coating was measured by micro Vickers hardness tester, and its microstructure was observed by SEM. Ten points were selected on the surface of every sample to measure the microhardness. During data processing the highest and lowest values were removed and the average value was taken as the final hardness value of the composite coating.

In this study, MG-2000 high-speed high-temperature friction and wear testing machine was used to conduct the friction and wear test of the composite coating. The wear resistance of coating was determined by measuring the amount of the reduction of the plating coating. The load was 10 N, speed 200 r/min and loading time 30 min. The size of the friction pair and sample was shown in Figure 1.

Electrochemical impedance spectroscopy (EIS) was used to evaluate the barrier properties of nano-containers of the coating. EIS measurements were conducted by an EG&G Parstat 2273 using a traditional three-electrode system. The coated sample with an exposure area of 1.0 cm^2 was used as the working electrode. A saturated calomel electrode (SCE, 0.242 V vs. SHE) was used as the reference

electrode (RE) and the coil-shaped platinum wire as the counter electrode. All potentials are referred to the SCE.

The impedance spectra were acquired at open-circuit potential (OCP) over the frequency range of 10^5- 10^{-2} Hz using an AC signal amplitude of 10 mV (rms). The validation of the impedance spectra was performed by checking the linearity condition.

3. RESULTS AND DISCUSSION
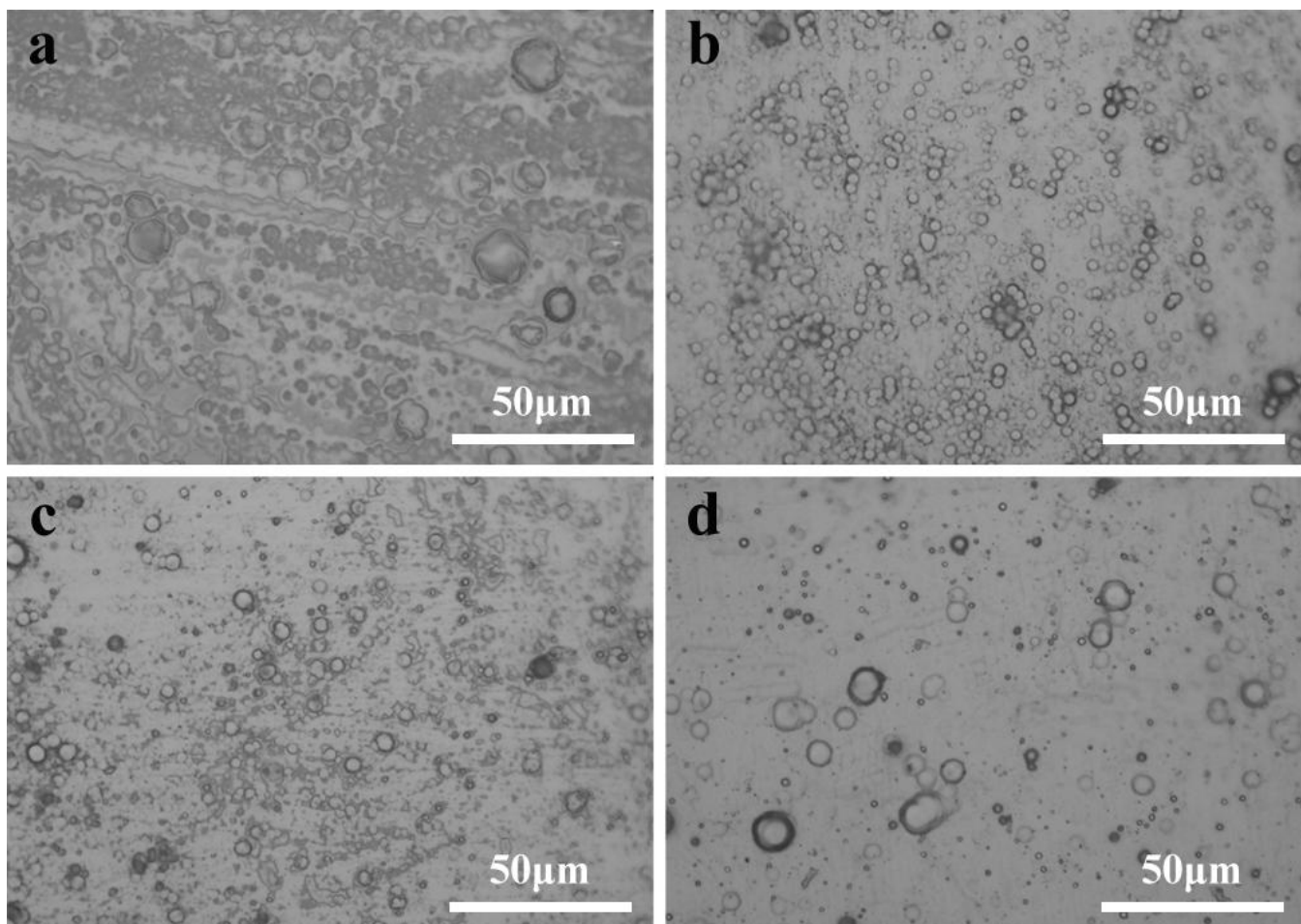
Figure 2. The metallographic of different CNTs content coating (a)Ni-P coating, (b) coating of 0.5g/L CNTs, (c) coating of 1.0g/L CNTs, (d) coating of 1.5g/L CNTs

The morphology of the surface of the coating sample was characterized by a JSM-6700F scanning electron microscopy (SEM) and an OLYMPUS DP12 optical microscope (OM).

The appearance of Ni-P coating and Ni-P-CNTs coating are bright, while the appearance becomes dimmer with the increase of CNTs. Figure 2 shows the metallographic of coatings of different CNTs concentration.

As shown in Figure 2, the deposited metal particles are coarse, the density of the surface is poor and there is a large gap between the particles on the surface of the Ni-P plating. The deposited metal

particles on the surface of Ni-P-CNTs composite coating are relatively smaller, and the density of the surface is much better than the Ni-P plating layer. The larger size of the metal particles on the coating surface became less and less, while the surface density was getting better and better with the increase concentration of CNTs as shown in Figure (d). This is because more and more CNTs were filled into the gaps between the deposited metal particles with the increase of the CNTs, so the surface density of the coating became significantly larger. Another phenomenon can also be observed from Figure (d): due to the easy aggregation of CNTs, the number of large size particles decrease, but the size increases. CNTs are tube bending so they are more easily aggregated together and filled the gaps between the deposited metal particles which cut off the interaction between the metal particles.
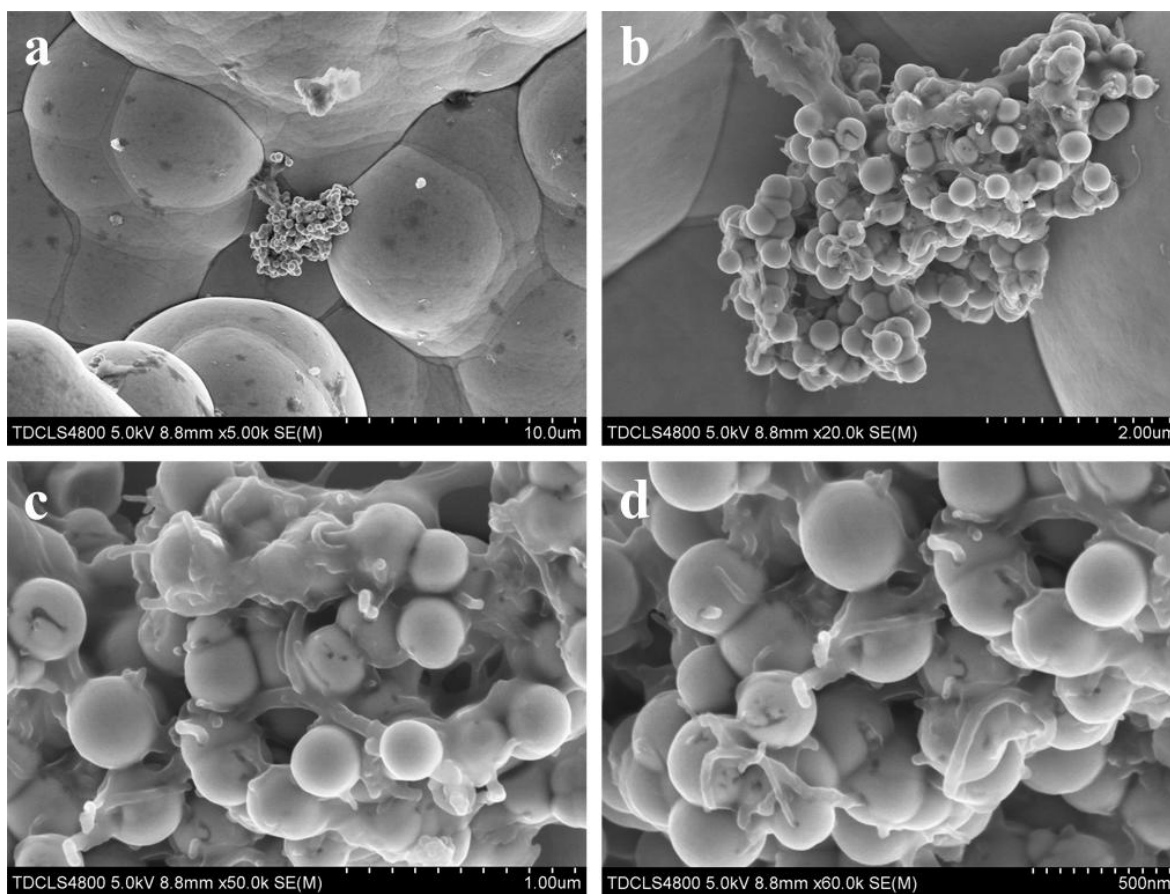
Figure 3. CNTs SEM imagines of different magnifications of 0.5g/L CNTs coating (a) magnification×5.00K, (b) magnification×20.0K, (c) magnification×50.0K, (d) magnification×60.0K

CNTs aggregate into a circular, and set the metal in circular individually isolated forming the "islands" morphology, which will be discussed later in corrosion resistance part of carbon nanotube composite coatings.

CNTs SEM images of different magnifications of 0.5 g•L^{-1} CNTs coating are shown in Figure 3. Figure 3a shows CNTs wind the deposited particles of Ni and P and deposit in the gap of the metal particles. As shown in Figure 3b-d, CNTs intersperse in the gaps between the deposited metal particles and the size of the metal particles is much smaller than the size of the metal particles which aren't

wrapped with CNTs. The codeposition of Ni-P-CNTs can work as a kind of lubricant between the coating and the other friction body. The wear resistance of the coating can be improved.
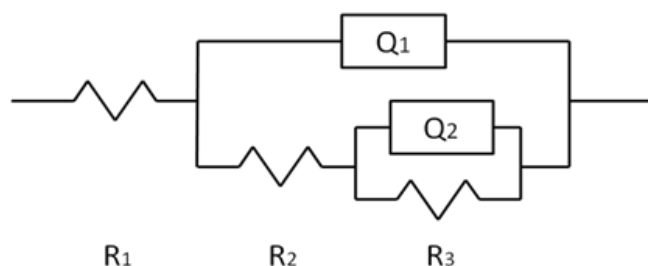
Figure 4. Equivalent circuit model for the Ni–P coating layers, where R_1 is electrolyte resistance, R_2 is coating layers resistance, R_3 is charge transfer resistance, Q_1 is coating layers constant phase element, and Q_2 is double layer constant phase element
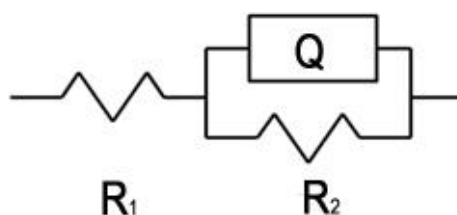
Figure 5. Equivalent circuit model for the Ni–P-nanoparticle coating layers, where R_1 is electrolyte resistance, R_2 is coating layers resistance, Q is coating layers constant phase element

A concentration of 3.5 wt% NaCl solution was used as a medium for rapid laboratory testing to test the corrosion resistance. After the composite plating of Ni-P, nickel-plated layer is cathodic plating as the standard potential of nickel is more positive than iron. During the plating process pores are generate more easily in the plating and the solution can penetrate through the pores to the iron base. The equivalent electrical circuit model in Figure 4 for EIS of the coating and the iron base exposed in the 3.5 wt% NaCl solution can be used to characterize the corrosion system, where R_1 is electrolyte resistance, R_2 is coating layers resistance, R_3 is charge transfer resistance, Q_1 is coating layers constant phase element, and Q_2 is double layer constant phase element.

After the composite plating of Ni-P-CNTs, nanoparticles deposited on the surface of the metal with Ni, P and nanoparticles are filled into the pores of the coating. The coating becomes dense and isolates the solution with the iron base. The equivalent electrical circuit model in Figure 5 for EIS of the coating and the iron base exposed in the 3.5 wt% NaCl solution can be used to characterize the corrosion system.
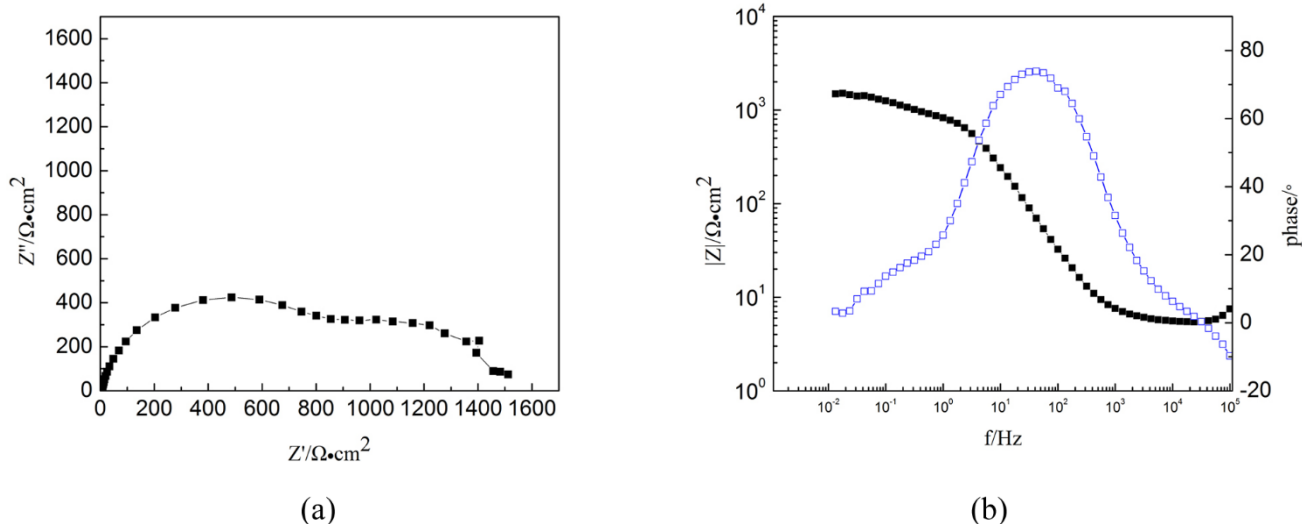
Figure 6. EIS of Ni-P coating: (a) Nyquist plot, (b) Bode plot
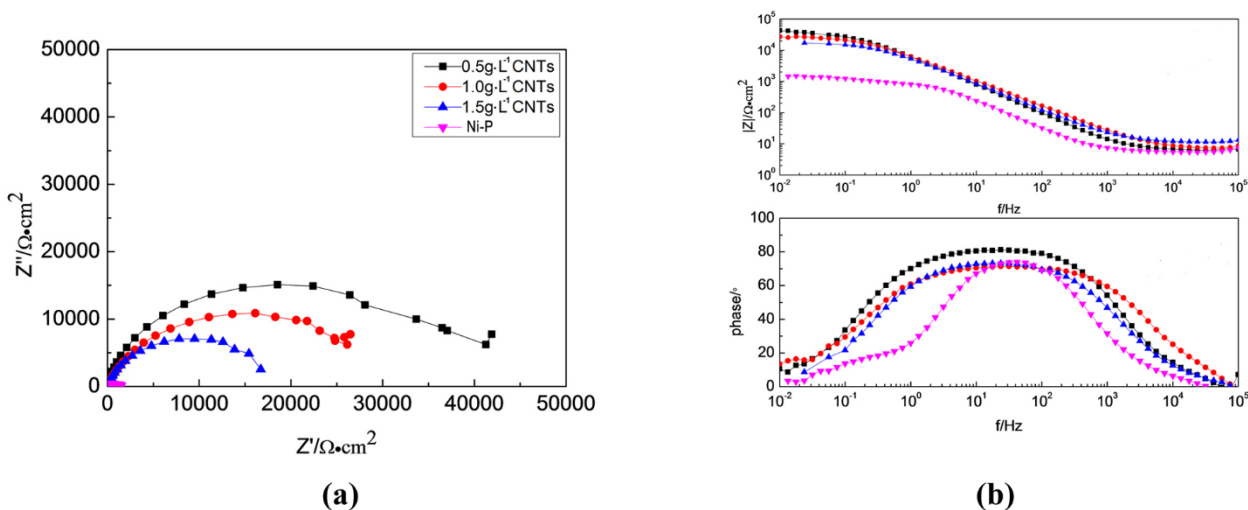
Figure 7. Effect of CNTs concentration on EIS: (a) Nyquist plot, (b) Bode plot

The plated samples were soaked in the 3.5 wt% NaCl solution for half an hour. Then the electrochemical impedance spectroscopy (EIS) and polarization curves were tested. The EIS data is shown in Figure 6 and 7.

As shown in Figure 6, the Nyquist curve of Ni-P plating has two capacitive arcs, which describes the solution has contacted the metal base through the gap of the plating and the charge transfer has occurred.

Figure 7 presents the comparison of EIS plots acquired at OCP of Ni-P-CNTs plating. The Nyquist curve of the composite coating with the co-deposition of CNTs has only one capacitive loop and the capacitive arc radius is bigger than the nickel-phosphorus plating. The Bode curve displays the impedance modulus |Z| of the composite coating is higher than the Ni-P plating, especially in the low

frequency region. Because the size of the nickel and phosphorus particles is large, an amount of pores and microscopic voids form in the plating of co-deposition of nickel-phosphorous. Thus the surface of the coating is not dense enough. Corrosion tends to occur in the area where the pores and microscopic voids exist. CNTs are well co-deposited with the metal particles onto the surface of the coating which form on the substrate because of the nanometer scale size of the carbon nanotubes. CNTs are widely distributed in the gaps of nickel and phosphorus and the coating is very dense.

Meanwhile, with the increase of the CNTs concentration, the capacitive arc radius of the coating decreases and the impedance modulus |Z| gradually decreases, indicating that the corrosion resistance of composite coatings get worse with the increase of CNTs concentration. This result is due to the tubular structure of CNTs. CNTs are carbon-related materials with nanometer diameter and perfect hollow molecular structure. CNTs are inclined to agglomerate. Too much CNTs deposite on the substrate and occupy the position of the nickel and phosphorus, leading to a large area of the carbon nanotubes wrapped together. This is very unfavorable to coating, resulting in the corrosion resistance of the coating reducing.

Table. 2 The calculated coating layers resistance and CPE parameters of coating layers (different CNTs concentration)

CNTs /g·L^{-1}	Q$_1$ /F·cm^2	R$_2$/Ω·cm^2
0	8.721E-5	963.6
0.5	3.013E-5	38620
1.0	3.372E-5	29020
1.5	3.615E-5	18080

Table 2 summarizes Q_1 and R_2 obtained by extrapolating impedance modulus. R_2 is coating layers resistance and Q_1 is coating layers constant phase element. R_2 can be used to characterize the corrosion resistance of the coating. The lower the value of R_2 is, the poorer the corrosion resistance is.

Figure 8 displays with the increase of the CNTs concentration coating resistance R_2 increases to the maximum and then decreases. When the concentration reaches at 0.5 g•L^{-1} R_2 has a maximum value. With the increase of the CNTs concentration Q_1 decreases to the minimum and then increases. But the increasing is small. Compared to the Ni-P coating without CNTs, Q_1 of the composite coating is smaller. Q_1 displays the uniformity of the coating. The smaller Q_1 is, denser the coating is. These results may be attributed to the role of the CNTs in modifying the structure. The nanoscale deposited CNTs reduce the surface and structural defects by filling the crevices, gaps and micron holes of the coating [24,27].

Considering R_2 and Q_1, it is concluded that the coating has a higher coating resistance and a better coating uniformity at the concentration of 0.5 g•L^{-1} CNTs. The combination of the coating and the substrate is the best at this concentration.

(a)   (b)
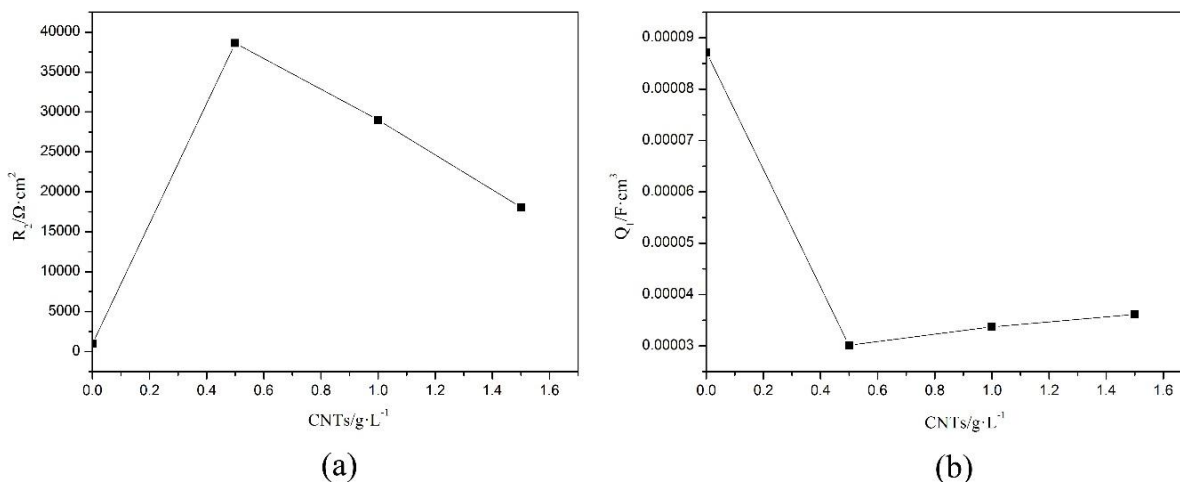
Figure 8. (a) Relation between the concentration of CNTs and R_2, (b) Relation between the concentration of CNTs and Q_1

After plated in the bath of different CNTs concentrations, the samples were soaked in a 3.5 wt% NaCl solution for half an hour. Then the polarization curves were measured. Figure 9 shows the effect of CNTs on polarization curve. Table 3 shows the corrosion potential of layers with different CNTs concentration.

Table. 3 Corrosion potential (V vs. SCE) of layers with different CNTs concentration

Coating type	Ni-P	0.5 g·L^{-1} CNTs	1.0 g·L^{-1} CNTs	1.5 g·L^{-1} CNTs
Ecorr/V	-0.5282	-0.3227	-0.3719	-0.3729
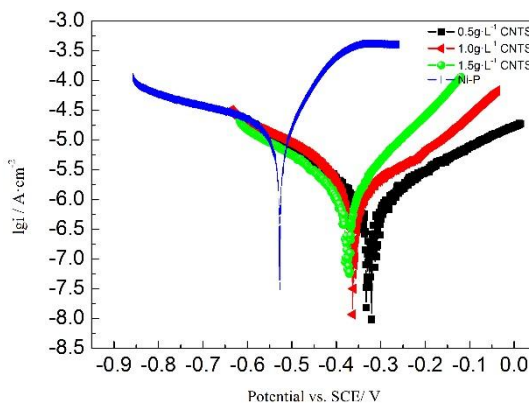
Figure 9. Effect of CNTs concentration on polarization curve

Corrosion potential of layers with different CNTs concentration was got from Figure 9. The corrosion potential （Ecorr）is the voltage difference between a metal immersed in a given

environment and an appropriate standard reference electrode. The more negative Ecorr is, the more the corrosion tendency is. The specific data is shown in Table 3.

As shown in Figure 9, the anodic Tafel curve in the anodic region changes, indicating the anodic reaction has changed. At the CNTs concentration of 0.5 g•L^{-1} the corrosion potential of Ni-P-CNTs composite coating is -0.3227 V vs. SCE and the corrosion potential of Ni-P coating is -0.5282 V vs. SCE. The potential moves negatively, showing the effect of anodic coating. With the increase of the CNTs concentration, the corrosion potential of the composite coating becomes negative gradually, indicating the corrosion resistance of the composite coating becomes worse. The conclusion from electrochemical impedance spectroscopy analysis coincides with the polarization curves analysis. It has been confirmed by other researchers [24, 25]. Contrary to our results it has been reported for Ni-P-CNTs coatings that microstructure of the Ni-CNT coatings became porous and with increase of the CNT concentration in the solution the corrosion resistance become worse with incorporation of CNTs into the coating [26].
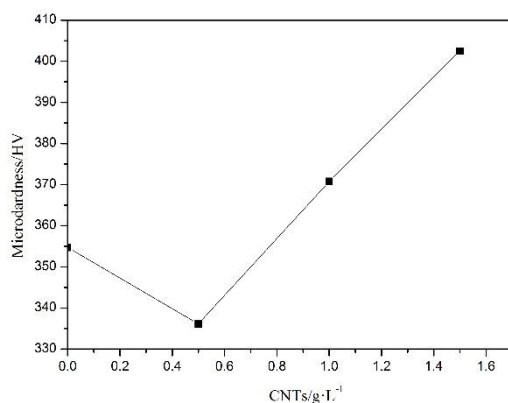
Figure 10. Average microhardness (HV) of layers with different CNTs concentration

The hardness of the composite coating was studied by means of micro Vickers hardness tester. Ten points on the surface of every specimen were measured. During post-processing, the highest and lowest values were removed and the average was taken as the final hardness value of the composite coating . To reduce the error, the average micro hardness was used to compare, as shown in Figure 10.

As shown in Figure 10, with the increase of the CNTs concentration the micro hardness of the Ni-P-CNTs composite coating decreases to the minimum and then increases. When the CNTs concentration is low, a relatively dense composite coating can't form and the CNTs hinder the codeposition of metal particles. Thus the hardness is lower than Ni-P coating. With the increase of the CNTs concentration the composite coating becomes denser and the hardness of CNTs is close to the hardness of diamond. The hardness of the coating increases meanwhile. It can be concluded that doping CNTs contributes to the micro hardness of the coating. Different with our results Wang said the hardness of the composite coatings increases with increase of the volume fraction of CNTs, but then decreases with further increasing the volume fraction [22].

After the wear test the lost volume of layers with different CNTs concentration is calculated by the wearing area and depth. The wearing volume V_{lost} is used to evaluate the wearing performance of the composite coating. Figure 11 shows the effect of CNTs concentration on the wear resistance.

As shown in Figure 11, with the increase of the CNTs concentration the lost volume V_{lost} of the Ni-P-CNTs composite coating in the friction and wear test decreases and is lower than that of Ni-P coating. It corresponds to the results from the microstructure of the Ni-P-CNTs composite coatings. The deposited metal particles are coarse, the density of the surface is poor and there is a large gap between the particles on the surface of the Ni-P plating. But the metal particles deposited on the surface of the Ni-P-CNTs composite coating are smaller and the gaps between the particles are filled with CNTs. The density of the Ni-P-CNTs composite coating is better than that of the Ni-P coating. With the increase of the CNTs concentration can function as grinding material better. According to some reports within the range of volume fraction of CNTs from 0 to 11.2%, the wear rate of the composite coatings showed a steadily decreasing trend with increasing volume fraction of CNTs [22].
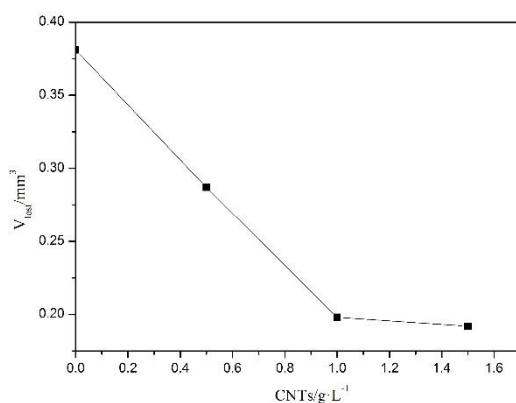
Figure 11. V_{lost} (mm^3）after friction of layers with different CNTs concentration

4. CONCLUSIONS

Electroless Ni–P–CNTs composite coating has been successfully deposited on a steel substrate from acidic bath containing CNTs.

1. The addition of CNTs makes the coating denser, thus compared with Ni-P coating, the corrosion resistance of composite coating is better. But too much CNTs deposited on the substrate occupy the position of the nickel and phosphorus, leading to a large area of the carbon nanotubes wrapped together which is very unfavorable to coating, resulting in the corrosion potential of the composite coating becoming negative gradually, indicating the corrosion resistance of the composite coating becomes worse. It achieves the best value when the CNTs concentration was 0.5 g·L^{-1}.

2. CNTs intersperse in the gaps between the deposited metal particles and the size of the metal particles is much smaller than the size of the metal particles which aren't wrapped with CNTs. The codeposition of Ni-P-CNTs can work as a kind of lubricant between the coating and the other friction

body. Compared to Ni-P coating, wear resistance and surface hardness value of Ni-P-CNTs coating are better, and they become much better with the increase of the CNTs concentration.

References

1. K. Ramani, D. Ramanujan, W. Z. Bernstein, F. Zhao, J. Sutherland, C. Handwerker, J.-K. Choi, H. Kim and D. Thurston, *J. Mech. Des.*, 132 (2010) 091004.
2. K. H. Krishnan, S. John, K. N. Srinivasan, J. Praveen, M. Ganesan and P. M. Kavimani, *Metal.l Mater. Trans. A*, 37A (2006) 1917.
3. X. Gan, K. Zhou, W. Hu and D. Zhang, *Surf. Coat. Technol.*, 206 (2012) 3405.
4. S. Mu, N. Li, D. Li and L. Xu, *Appl. Surf. Sci.*, 256 (2010) 4089.
5. P. Makkar, R. C. Agarwala and V. Agarwala, *Adv. Powder Technol.* 25(2014)1653.
6. N. Tsyntsaru, H. Cesiulis, E. Pellicer, J. P. Celis and J. Sort, *Electrochim. Acta*, 104 (2013) 94.
7. K. Chaiyaput, A. E.-M. Gamal., N. Atsushi, T. Tooru, Electrochemistry, 78 (2010) 188.
8. X. Hu, S. Xu, Y. Yang, Z. Chen and Y. C. Chan, *Mater. Sci. Eng., A*, 600 (2014) 67.
9. S. Karthikeyan and B. Ramamoorthy, *Appl. Surf. Sci.*, 307(2014) 654.
10. S. Rahmanian, A. R. Suraya, M. A. Shazed, R. Zahari and E. S. Zainudin, *Mater. Des.*, 60(2014) 34.
11. J.-D. Lin and C.-L. Kuo, *Surf. Coat. Technol.*, 209(2012) 80.
12. Y. Cheng, T. Li, C. Fang, P. Liu, R. Yu and J. Hu, *Composites Part B*, 47(2013) 290.
13. M. S. Gaur, R. Singh and R. K. Tiwari, *J. Electrostat.*, 72(2014) 242.
14. W. Li and W. Bauhofer, *Carbon*, 49(2011) 3891.
15. H. H. Kim, J. S. S. Babu and C. G. Kang, *Mater. Sci. Eng.*, 573(2013) 92.
16. S. A. Niaki and R. Naghdabadi, *Composites Part B*, 43(2012) 3167.
17. K. T. Lau and D. Hui, *Composites Part B*, 33(2002) 263.
18. E. T. Thostenson, Z. F. Ren and T. W. Chou, *Compos. Sci. Technol.*, 61(2001) 1899.
19. M. Loffler, U. Weissker, T. Muhl, T. Gemming and B. Buchner, *Ultramicroscopy*, 111(2011) 155.
20. M. B. Nardelli, B. I. Yakobson and J. Bernholc, *Phys. Rev. B:* Condens. Matter, 57(1998) R4277.
21. S. Berber, Y. K. Kwon and D. Tomanek, *Phys. Rev. Lett.*, 84(2000) 4613.
22. L. Y. Wang, J. P. Tu, W. X. Chen, Y. C. Wang, X. K. Liu, C. Olk, D. H. Cheng and X. B. Zhang, *Wear*, 254(2003)1289.
23. X.H. Chen, C.S. Chen, H.N. Xiao, F.Q. Cheng, G. Zhang, G.J. Yi, *Surf. Coat. Technol.*, 191 (2005)351.
24. M. Alishahi, S. M. Monirvaghefi, A. Saatchi and S. M. Hosseini, *Appl. Surf. Sci.*, 258(2012) 2439.
25. Y.L. Shi, Z. Yang, H. Xu, M.K. Li, H.L. Li, *J. Mater. Sci.*, 39 (2004) 5809.
26. S.-K. Kim and T.-S. Oh, *Trans. Nonferrous Met. Soc. China*, 21(2011)s68.
27. Z. Yang, H. Xu, M.K. Li, Y.L. Shi, Y. Huang, H.L. Li, *Thin Solid Films*, 466 (2004) 86.